

Lattice and perturbative QCD analysis of exclusive processes

Steven Gottlieb*

Department of Physics, University of California, San Diego, La Jolla, California 92093

Andreas S. Kronfeld†

Newman Laboratory of Nuclear Studies, Cornell University, Ithaca, New York 14853

(Received 10 July 1985)

We use the results of a Monte Carlo simulation of quantum chromodynamics in the quenched approximation to compute the first two moments of the π and ρ distribution amplitude. Our results turn out to be surprisingly large, and we discuss some of the phenomenological implications of this turn of events. In addition to the distribution amplitude itself, we predict the pion form factor and the cross section for $\gamma\gamma \rightarrow \pi^0\pi^0$, and we compare the former with experiment. We also contrast lattice-gauge-theory predictions with those of QCD sum rules.

I. INTRODUCTION

Detailed theoretical predictions in many areas of particle physics are limited because no one has calculated matrix elements with hadronic contributions.¹ However, the development of numerical algorithms² and special purpose computers³ indicates that lattice gauge theory will provide the basis needed for these calculations. In the meantime, it is worth remarking that many relevant matrix elements can be evaluated from existing Monte Carlo ensembles of gauge field configurations and their associated quark propagators. This article presents the results of such a calculation for the first two nonzero moments of the π - and ρ -meson distribution amplitude.

In perturbative quantum chromodynamics a wide variety of processes can be "factorized" into a convolution of perturbative scattering amplitudes and nonperturbative functions. The moments of the latter are hadronic matrix elements of local operators which appear in the operator-product expansion⁴ and which have been recently investigated in lattice gauge theory.⁵ Because the lattice theory breaks some of the invariances of the continuum theory, any naive lattice formulation of the operators introduces power-law divergences.⁶ Reference 5 shows how the divergences of the naive operators are related to operators of lower mass dimension and how to remove them by explicit subtraction. For example, to calculate the second moment one needs three counterterms in addition to the naive operator.

The distribution amplitude $\phi(x_i, Q)$ contains the non-perturbative information needed to predict exclusive scattering amplitudes at wide angles; in a physical gauge it is the probability amplitude for a hadron to consist of valence partons which have fractional momentum x_i and which are collinear up to scale Q . For mesons it is convenient to define $\zeta = x_q - x_{\bar{q}}$. Then the moments of the distribution amplitude

$$A^{(k)}(Q) \equiv \sqrt{2n_c} \int_{-1}^1 \zeta^k \phi(\zeta, Q) d\zeta \quad (1.1)$$

are proportional to matrix elements of local operators:

$$\langle 0 | O_{\mu_0\mu_1 \dots \mu_k}^{(k)} | h \rangle^{(Q)} = A^{(k)}(Q) (p_{\mu_0} \dots p_{\mu_k} - \text{traces}), \quad (1.2)$$

where Q is an ultraviolet cutoff in the theory, and

$$O_{\mu_0\mu_1 \dots \mu_k}^{(k)} = i^{-k} \bar{\psi} \Gamma_{\mu_0} \vec{D}_{\mu_1} \dots \vec{D}_{\mu_k} \psi - \text{traces}. \quad (1.3)$$

Here $\Gamma_\mu = \gamma_\mu \gamma_5 (\gamma_\mu)$ for the π and helicity-0 ρ mesons, respectively.

The lattice calculation can give the moments at only one specific value of Q , which is related to the lattice spacing, as explained in Ref. 5. To extend our calculation to all values of Q , one can use the renormalization group. The operators in Eq. (1.3) mix under the renormalization group, so it is convenient to diagonalize the anomalous dimension matrix and work with Gegenbauer moments,

$$\tilde{A}^{(n)} \equiv \sqrt{2n_c} \int_{-1}^1 C_n^{(3/2)}(\zeta) \phi(\zeta, Q) d\zeta \quad (1.4)$$

and associated operators,

$$\begin{aligned} \tilde{O}_{\mu_0\mu_1 \dots \mu_n}^{(n)} = & \sum_k^{[n/2]} b_{2k}^{(n)} i^{-(n-2k)} \partial_{\mu_{2k+1}} \dots \partial_{\mu_n} O_{\mu_0\mu_1 \dots \mu_{2k}}^{(2k)} \\ & - \text{traces}, \end{aligned} \quad (1.5)$$

where the $b_{2k}^{(n)}$ are the coefficients of the Gegenbauer polynomial,⁷ $C_n^{(3/2)}$. For these moments the renormalization group tells us that

$$\frac{\tilde{A}^{(n)}(Q)}{\tilde{A}^{(n)}(Q_0)} = \left[\frac{\ln(Q^2/\Lambda^2)}{\ln(Q_0^2/\Lambda^2)} \right]^{-\gamma_n/\beta_0}, \quad (1.6)$$

where γ_n is the one-loop anomalous dimension of $\tilde{O}^{(n)}$, and $\beta_0 = 11 - 2n_f/3$ is the one-loop coefficient of the β function. Equation (1.4) can be inverted to give the distribution amplitude in terms of the moments:⁸

$$\phi(\zeta, Q) = \sum_n \frac{\sqrt{2}(3+2n)}{\sqrt{n_c}(2+n)(1+n)} C_n^{(3/2)}(\zeta) \tilde{A}^{(n)}(Q), \quad (1.7)$$

a form which will be useful in phenomenological applica-

tions of our results.

We have computed the first two moments for the π and the ρ using 19 configurations of SU(3) Monte Carlo data at $\beta=5.7$ on a $6^2 \times 12 \times 18$ lattice. These data neglect the effects of quark vacuum polarization. We had quark propagators at three values of the hopping parameter: $K=0.325, 0.34,$ and 0.355 . Further details of the simulation have been published elsewhere.⁹

II. CALCULATION

A. Operators and notation

Since the operators of Eqs. (1.3) and (1.5) contain derivatives in the continuum theory, one must formulate a discretization prescription; we use the symmetric difference prescription of Ref. 5. To be specific

$$\partial_\mu = (2a)^{-1}(t_\mu - t_{-\mu}), \quad (2.1)$$

where $t_{\pm\mu}$ are translation operators which transport fields by one link in the $\pm\hat{\mu}$ direction. Similarly

$$\vec{D}_\mu = D_\mu - \bar{D}_\mu = (2a)^{-1}(T_\mu - T_{-\mu} + \bar{T}_\mu - \bar{T}_{-\mu}), \quad (2.2)$$

where the T 's transport fields covariantly, and the back arrow (\leftarrow) indicates that the operator acts on fields to its left. Using these definitions it is straightforward to expand the $O^{(n)}$ in terms of gauge field matrices U ; the re-

$$\begin{aligned} \langle 0 | O^{(2)} | \rho; h=0 \rangle^{(Q)} &= A_1^{(2)}(Q)(p \times p \times p - \text{traces}) + A_2^{(2)}(Q)(\epsilon \times p \times p - \text{traces})m_\rho \\ &+ A_3^{(2)}(Q)(\epsilon \times \epsilon \times p - \text{traces})m_\rho^2 + A_4^{(2)}(Q)(\epsilon \times \epsilon \times \epsilon - \text{traces})m_\rho^3. \end{aligned} \quad (2.6)$$

The continuum analysis⁸ requires the combination of the $A_i^{(2)}$ that is given by the $\mu=\nu=\lambda=+$ component.¹⁰ Furthermore, a helicity-0 vector meson has $\epsilon^+ - p^+ / m$ in any frame, so we have

$$\langle 0 | O^{(2)+++} | \rho; h=0 \rangle^{(Q)} = A^{(2)}(Q)(p^+)^3, \quad (2.7)$$

where

$$A^{(2)}(Q) = A_1^{(2)}(Q) + A_2^{(2)}(Q) + A_3^{(2)}(Q) + A_4^{(2)}(Q). \quad (2.8)$$

The power-law divergences of $O^{(2)+++}$, with $\Gamma=\gamma$, can be removed with

$$O_\mu^{(c)} = a^{-1} \bar{\psi} i^{-1} \vec{D}_\mu \psi, \quad (2.9a)$$

$$O_\mu^{(e)} = a^{-1} \partial^j \bar{\psi} \sigma_{\mu j} \psi, \quad (2.9b)$$

and

$$O_\mu^{(0)} = a^{-2} \bar{\psi} i \gamma_\mu \psi. \quad (2.9c)$$

O^{+++} can be written in terms of Cartesian components (we assume symmetrization of the indices):

$$O^{+++} = (O_{iii} - 3O_{00i}) + i(O_{000} - 3O_{0ii}). \quad (2.10)$$

sult for $O^{(2)}$ is exhibited in Ref. 5.

For the pion we considered the component of $O_{\mu\nu\lambda}^{(2)}$ with $\mu=\nu=\lambda=0$. Using the naive definitions of Eqs. (1.3) and (2.2) gives an operator with power-law divergences. These can be removed by

$$O^{(c)} = a^{-1} \bar{\psi} \sigma_{0j} \gamma_5 \vec{D}^j \psi, \quad (2.3a)$$

$$O^{(e)} = a^{-1} i^{-1} \partial_0 \bar{\psi} \gamma_5 \psi, \quad (2.3b)$$

and

$$O^{(0)} = a^{-2} \bar{\psi} i \gamma_0 \gamma_5 \psi. \quad (2.3c)$$

The results of Ref. 5 show that

$$O_R^{(2)} = O_U^{(2)} - C_F \frac{\alpha}{4\pi} (1.58O^{(c)} + 4.83O^{(e)} + 2.58O^{(0)}) \quad (2.4)$$

is free of power-law divergences to $O(\alpha)$. [The coefficients in Eq. (2.4) may seem large, but we point out that $C_F \alpha / 4\pi = 8.9 \times 10^{-3}$ for $\beta=5.7$.] Finally, from Eq. (1.2), the moment, $A^{(2)}(Q)$, is related to $O_R^{(2)}$ by

$$\langle 0 | O_R^{(2)} | \pi \rangle^{(Q)} = A^{(2)}(Q) (\frac{1}{2} p_0^3). \quad (2.5)$$

(The factor $\frac{1}{2}$ is due to the trace term.)

The case of the helicity-0 ρ meson is slightly more complicated because the polarization vector ϵ makes the tensor decomposition of Eq. (1.2) incorrect. If one makes no dynamical assumptions the correct decomposition is

Our numerical calculation indicates that the ‘‘imaginary part’’ is consistent with zero. Repeating the calculations of Ref. 5 for the ‘‘real part’’ yields the result that

$$O_R^{(2)} = O_U^{(2)} - C_F \frac{\alpha}{4\pi} (-13.69O^{(c)} + 9.57O^{(e)} + 4.28O^{(0)}) \quad (2.11)$$

is free of power-law divergences to $O(\alpha)$.

B. Matrix elements

To calculate a matrix element of a local operator, $\langle 0 | O^{(n)} | \pi \rangle$, for $n=0,2,c,e$, consider the correlation function

$$C^{(n)}(t) = \sum_{\mathbf{x}} \langle O^{(n)}(\mathbf{x}, t) O^{(0)\dagger}(\mathbf{0}, 0) \rangle. \quad (2.12)$$

Inserting a complete set of relativistically normalized states yields

$$C^{(n)}(t) = \sum_j (2m_j)^{-1} \langle 0 | O^{(n)} | j \rangle \langle j | O^{(0)\dagger} | 0 \rangle F(m_j, t), \quad (2.13)$$

where

$$\begin{aligned}
F(m,t) &= e^{-mt} + e^{-m(N_4-t)} \\
&= 2e^{-mN_4/2} \cosh[m(\frac{1}{2}N_4-t)]
\end{aligned}
\quad (2.14)$$

reflects the periodicity in the time direction, whose axis has length N_4 . If the radial excitations, $j > 1$, have large enough masses, $C^{(n)}$ should be well approximated, near $t = N_4/2$, by two terms:

$$C^{(n)}(t) = M_1^{(n)} M_1^{(0)*} \frac{F(m_1,t)}{2m_1} + M_2^{(n)} M_2^{(0)*} \frac{F(m_2,t)}{2m_2}, \quad (2.15)$$

where the M 's are abbreviations for the matrix elements.

Once the correlation functions have been computed from the numerical simulation, one can fit them to the shape indicated by Eq. (2.15) to determine the masses, and the coefficients of the functions F . From the latter the matrix elements can be extracted. We have done this for $C^{(0)}$, $C^{(2)}$, $C^{(c)}$, and $C^{(e)}$. For $C^{(0)}$ this analysis is quite straightforward; we obtain the same value for the matrix element when we throw out the first 3, 4, or 5 time slices. Unfortunately we are not so successful on the other correlation functions, which is probably a consequence of the notorious problems¹¹ in fitting the expression in Eq. (2.15). We find adequate fits for a wide range of different values of m_2 and of the M 's.

However, once a particular matrix element, say, $M_1^{(0)}$, has been determined satisfactorily, it is actually unnecessary to rely on any fitting procedures to predict, say, $M_1^{(2)}$. If one takes the ratio of two correlation functions, one obtains, near $t = N_4/2$, where $F(m_2,t)/F(m_1,t)$ is small,

$$\begin{aligned}
R^{(n)}(t) &\equiv \frac{C^{(n)}(t)}{C^{(0)}(t)} \\
&= \frac{M_1^{(n)}}{M_1^{(0)}} \left[1 + \frac{m_1}{m_2} \frac{M_2^{(0)*}}{M_1^{(0)*}} \frac{F(m_2,t)}{F(m_1,t)} \right. \\
&\quad \left. \times \left[\frac{M_2^{(n)}}{M_1^{(n)}} - \frac{M_2^{(0)}}{M_1^{(0)}} \right] \right]. \quad (2.16)
\end{aligned}$$

For our time axis, $N_4 = 18$, and for the masses that emerge from fitting $C^{(0)}$ the second term in the large square bracket is negligible for $t > 6(8)$ for the $\pi(\rho)$ meson. Hence the desired matrix element, $M_1^{(n)}$, can be deduced from the ratio, $R^{(n)}(t)$, near $t = N_4/2$, and the (theoretical or experimental) knowledge of $M_1^{(0)}$. In the following we will denote by $R^{(n)}$, without the explicit time argument, the ratio $M_1^{(n)}/M_1^{(0)}$.

III. RESULTS

Unfortunately it is impossible¹² to compute quark propagators numerically near physical values of K , and one must extrapolate to that value K_p to obtain honest results. We determine K_p by assuming that m_π^2 is linear in K and tuning to $m_\pi = 140$ MeV. To do this one needs the value of the lattice spacing in physical units. Using the string tension as input implies $a = 0.993$ (MeV)⁻¹; the alterna-

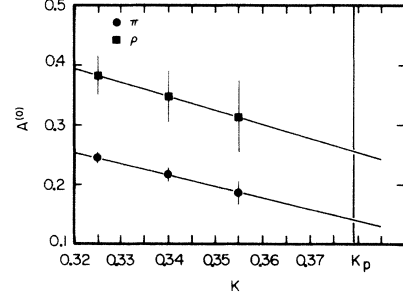


FIG. 1. Zeroth moment $A^{(0)}$ of the π and ρ distribution amplitudes as a function of K , extrapolated to the physical value $K_p = 0.379$. Circles denote numerical data for the π and squares the ρ .

tive procedure of using (m_π, f_π) to determine (K_p, a) gives the same answers for this simulation.

The first moment of the distribution amplitude is proportional to weak or electromagnetic decay constants:

$$A_\pi^{(0)} = \sqrt{2} f_\pi, \quad A_\rho^{(0)} = 2 f_\rho. \quad (3.1)$$

Linear fits of these quantities for the three values of K are shown in Fig. 1, and agree very well with experiment: $A_\pi^{(0)} = 139$ MeV (expt. 132 MeV) and $A_\rho^{(0)} = 252$ MeV (expt. 214 MeV).

For the second moment it is sensible to extrapolate one whose expected K dependence is mild. First, one should remove the power-law divergences at the unphysical values of K in case the size of the “finite” part is set by the pion mass. Tables I and II, respectively, for the π and ρ , show the three ratios of matrix elements needed to do this, as well as the combination, given by Eqs. (2.4) and (2.11), that is free of divergences to $O(a)$. From Eqs. (2.5) and (2.7) one expects these ratios to be proportional to m^3 in the continuum limit, and hence quite strongly dependent on K . To account for $O(a^2)$ terms one can interpret the p^0 on the right-hand sides of these formulas as $\sin p^0 = i \sinh m$. This would be correct for a $\bar{q}q$ state in a free Euclidean lattice theory. Then one can use Eqs. (2.5) and (2.7) to determine $A_R^{(2)}$ as a function of K . From Fig. 2, which is a plot of $A_R^{(2)}$ vs K , we obtain $A_\pi^{(2)} = 233$ MeV and $A_\rho^{(2)} = 259$ MeV. We have also fitted the ratio of moments, $A_R^{(2)}/A^{(0)}$, to straight lines, which is shown in Fig. 3. The results are somewhat smaller than those from Fig.

TABLE I. Raw results for the ratio of π correlation function, and the ratio that is free of power-law divergences.

K	$R^{(2)}$	$R^{(c)}$	$R^{(e)}$	$R_R^{(2)}$
0.325	-0.970(30)	-2.785(50)	-3.65(15)	-0.797(30)
0.340	-0.875(30)	-2.861(50)	-3.48(15)	-0.709(30)
0.355	-0.772(30)	-2.91(10)	-3.31(15)	-0.612(30)

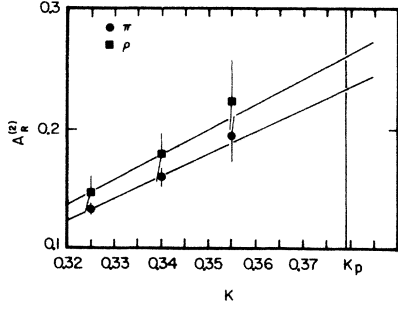


FIG. 2. Second moment $A_R^{(2)}$ of the π and ρ distribution amplitudes as a function of K , extrapolated to the physical value $K_p=0.379$. Circles denote numerical data for the π and squares the ρ . These data have power-law divergences removed as indicated by Eqs. (6.2) and (6.9).

$2-A_\pi^{(2)}=191$ MeV and $A_\rho^{(2)}=235$ MeV; however, the statistical error alone is about 20 MeV for the numbers quoted here, so both methods agree.¹³ Finally, the relationship between the continuum scale Q and the lattice spacing⁵ implies that $Q=7.5$ GeV for the π , and $Q=6.8$ GeV for the ρ .

Numerical values for various quantities are in Tables III and IV for the π and ρ , respectively. Careful readers will notice that the column labeled $A_R^{(2)}/A^{(0)}$ is not quite the ratio of the columns labeled $A_R^{(2)}$ and $A^{(0)}$. This is because we determined the ratio by computing directly

$$\frac{A_R^{(2)}}{A^{(0)}} = \frac{C_R^{(2)}}{(-i\partial_0)^2 C^{(0)}}, \quad (3.2)$$

which mimics the continuum analysis where the parton momentum (\vec{D}) is scaled by the total momentum (∂).

We have also used the Monte Carlo data to compute $\langle 0|O^{(1)}|\pi\rangle$ and $\langle 0|O^{(1)}|\rho\rangle$ which should vanish by charge-conjugation invariance. The associated correlation functions $C^{(1)}$ are smaller than $C^{(0)}$ and $C^{(2)}$ by 2 orders of magnitude, and they fluctuate in sign as a function of t . We therefore conclude that the matrix elements are consistent with zero.

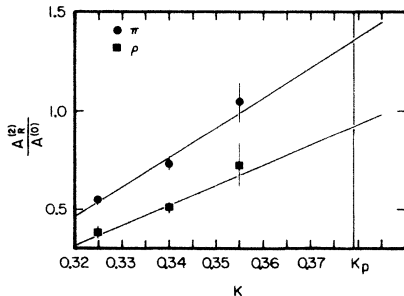


FIG. 3. The ratio of moments $A_R^{(2)}/A^{(0)}$ determined from the ratio of correlation functions in Eq. (6.16).

TABLE II. Raw results for the ratio of ρ correlation functions, and the ratio that is free of power-law divergences.

K	$R_U^{(2)}$	$R^{(c)}$	$R^{(e)}$	$R_R^{(2)}$
0.325	-0.501(2)	-0.760(10)	0.961(1)	-0.713(5)
0.340	-0.469(2)	-0.772(10)	0.787(1)	-0.668(5)
0.355	-0.459(10)	-0.782(10)	0.635(1)	-0.646(12)

Some authors¹⁴ prefer to extrapolate in $1/K$; we have done this also and found that the quality of the fit is not as good. The numerical values of our results change by at most 1% when we adopt this strategy.

IV. AN ENCOUNTER WITH EXPERIMENTS

The values we have obtained for the second moments are large, indeed radically so. For ground-state mesons one might expect, by analogy with nonrelativistic quantum mechanics, ϕ to have no nodes in the interval $-1 < \xi < 1$, although this attitude is certainly not well founded. However, our calculation insists that the π distribution amplitude has a zero because

$$A^{(2)}/A^{(0)} = \int \xi^2 \phi d\xi / \int \phi d\xi > 1,$$

and it suggests very strongly that the ρ distribution amplitude has one as well. We have illustrated this in Fig. 4, which shows the asymptotic distribution amplitude along with those based on our results for the pion and the assumption that the higher ($n \geq 4$) moments in Eq. (1.7) are negligible. Although that assumption is untenable, the conclusion that the distribution amplitude differs greatly from the asymptotic shape, even at high Q^2 , is inescapable.

In the following we will continue to concentrate on the pion, rather than the ρ , because the character of our experimental predictions would be quite similar in both cases, and because the pion is easier to identify in experiments.

The most accessible experimental data that might test the theoretical calculation is the pion form factor. Lepage and Brodsky⁸ have shown that at large Q^2

TABLE III. Results for the π extrapolated to the physical value of K . All quantities are dimensionless; physical units can be restored using $a=993$ (MeV)⁻¹.

K	m_π^2	$A_\pi^{(0)}$	$A_\pi^{(2)}$	$\frac{A_\pi^{(2)}}{A_\pi^{(0)}}$
0.325	1.000(40)	0.243(8)	0.133(5)	0.547(20)
0.340	0.723(34)	0.215(13)	0.159(8)	0.735(40)
0.355	0.476(55)	0.184(20)	0.192(20)	1.05(10)
0.379(5)	yields K_p	0.140(28)	0.235(25)	1.37(20)
Experiment	0.020	0.133		

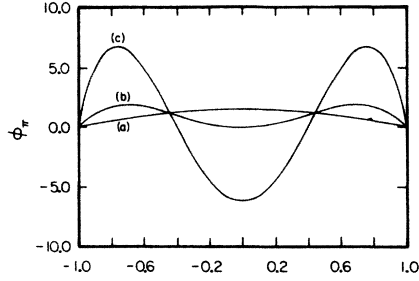


FIG. 4. The π distribution amplitude for various values of $\tilde{A}_R^{(2)}(Q)$. (a) The asymptotic result $\tilde{A}_R^{(2)}(Q)=0$. (b) The result from QCD sum rules, Ref. 15, that worked at $Q=0.5$ GeV. (c) The result of the present numerical work, using the method of Fig. 2; $Q=7.5$ GeV. Using Eq. (1.6) to reconcile the momentum scales increases the discrepancy between curves (b) and (c).

$$Q^2 F_\pi(Q^2) = C_F \frac{8\pi}{n_c} \alpha_s(Q^2) \left| \sum_{n \text{ even}} \frac{2n+3}{(2+n)(1+n)} \tilde{A}^{(n)}(Q) \right|^2$$

$$= 16\pi f_\pi^2 \alpha_s(Q^2) \left[1 + \frac{7}{18} \frac{\tilde{A}^{(2)}(Q)}{A^{(0)}} + \dots \right]^2, \quad (4.1)$$

where on the second line we have set $n_c=3$ and $C_F=\frac{4}{3}$. As shown in Fig. 5, the theoretical prediction is too small when the second and higher moments are neglected; however, it is too large when only the second is included. One possibility, of course, is that a higher moment has the opposite sign and thus reduces the right-hand side of Eq. (4.1) to phenomenologically acceptable levels.

We have also predicted the cross section for $\gamma\gamma \rightarrow \pi^0\pi^0$. In perturbative QCD that cross section¹⁸ is

$$\frac{d\sigma}{dt} = \frac{200\pi\alpha_{EM}^2}{81} \left| \frac{F_\pi(s)}{s} \right|^2 g^2[\theta_{c.m.}; \phi_\pi]. \quad (4.2)$$

The dependence on the distribution amplitude is in the form factor F_π and g , which is a functional of ϕ and a function of the center-of-mass scattering angle $\theta_{c.m.}$. For an explicit formula, see Ref. 18. Unlike F_π , g has no sim-

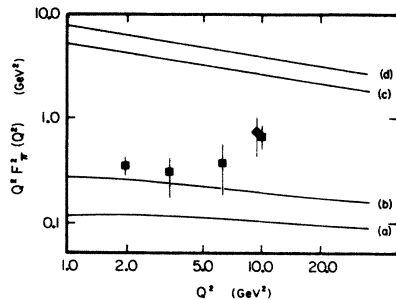


FIG. 5. The pion form factor. (a) Asymptotic theoretical prediction. (b) QCD sum-rule prediction. (c) and (d) The prediction of the present work, assuming that higher moments are negligible (they are not), using Figs. 3 and 2, respectively. The points are from $ep \rightarrow en\pi^+$ (squares, Ref. 16) and $\psi \rightarrow \pi^+\pi^-$ (diamond, Ref. 17). We present both of our extrapolations here to give some indication of the systematic (and statistical) errors in our calculation.

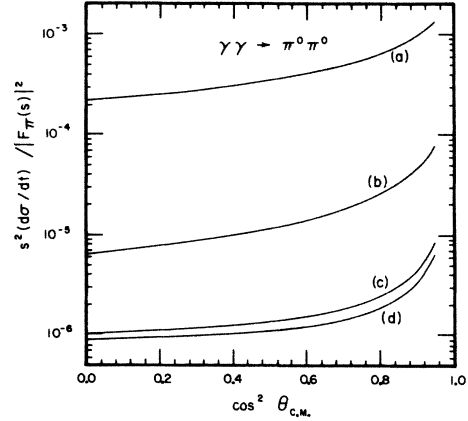


FIG. 6. Cross section for $\gamma\gamma \rightarrow \pi^0\pi^0$, scaled by the form factor as suggested in Ref. 18. Curves (a)–(d) correspond to the methods listed in Fig. 5.

ple expression in terms of the moments; indeed we performed the necessary convolutions numerically for each value of $\theta_{c.m.}$. In Fig. 6 we have plotted this cross section as a function of $\cos^2\theta_{c.m.}$ with the form-factor dependence removed.¹⁹

These moments have also been evaluated with QCD sum rules,¹⁵ and the results are rather smaller than ours. For example, the sum rules yield $A^{(2)}(Q=0.5 \text{ GeV}) = 0.46 A^{(0)}$ for the pion, whereas we have [using Eq. (1.6) and taking $\Lambda_{\overline{MS}}=0.1 \text{ GeV}$] $A^{(2)}(Q=0.5 \text{ GeV}) = 2.92 A^{(0)}$. The dramatic disagreement between the two methods warrants some comment. Although QCD sum rules agree impressively with a variety of experimental data, including the pion form factor, as seen in Fig. 5, and heavy-meson decays to π pairs, their derivation is not entirely rigorous. Moreover, the model distribution amplitude, $\phi \sim \xi^2(1-\xi^2)$, proposed in Ref. 15 to reproduce the moments calculated from the sum rules, implies that there is no probability of the quark and antiquark sharing the meson momentum equally. This would be a very striking and counterintuitive situation.

On the other hand, the distribution amplitude shown in Fig. 4 indicates a large probability of equal sharing, as well as a significant probability of skewed sharing. This observation still holds if one introduces into the distribu-

TABLE IV. Results for the ρ extrapolated to the physical value of K . All quantities are dimensionless; physical units can be restored using $a=993 \text{ (MeV)}^{-1}$.

K	m_ρ	$A_\rho^{(0)}$	$A_\rho^{(2)}$	$\frac{A_\rho^{(2)}}{A_\rho^{(0)}}$
0.325	1.07(4)	0.382(32)	0.146(14)	0.383(30)
0.340	0.94(5)	0.346(44)	0.176(20)	0.507(30)
0.355	0.81(4)	0.312(60)	0.229(30)	0.73(11)
0.379	0.60(9)	0.254(110)	0.261(50)	0.933(20)
Experiment	0.775	0.216		

tion amplitude of Fig. 4 higher moments, $\tilde{A}^{(n)}$, $n \geq 4$, of the appropriate magnitudes and signs to obtain agreement with the form-factor pair-production data. The distribution amplitude that would emerge from playing with the higher moments in this way would have many nodes, a structure which would arise if the meson's constituents were constrained by a boundary but otherwise free.²⁰

Instead of drawing profound conclusions, however, we should note that there are several aspects inherent to any Monte Carlo lattice gauge theory calculation which may lead to systematic errors. These include the mass extrapolations in Figs. 1–3 due to the failure at small mass of the quark propagator algorithm, finite-size effects due to the finite box that must be used, and finite-lattice-spacing effects related to the value of the coupling constant. Also, we cannot be certain that $\beta=5.7$ is a sufficiently weak coupling that the one-loop scaling formula, Eq. (1.6), holds. If not, the Q^2 evolution in Figs. 5(c) and 5(d) would be modified, not only because of a different scaling law, but also because of higher twist effects, which we have neglected. Finally, it is important to note that these calculations were done in the quenched, or valence, approximation.²¹ Hence, it is clear that there are many possibilities to improve these calculations, and that such improvements ought to be incorporated as simulations of QCD become more refined.

V. SUMMARY AND CONCLUSIONS

Because it determines only two nontrivial moments, the numerical study of the meson distribution amplitudes presented here is far from complete and, hence, not yet quite compatible with experimental data. Nevertheless, it does provide some physical insight to hadronic structure. Reference 5 argued that the size of the counterterms is related to the separation of the valence quarks; for example, for $O^{(2)}$ and its most severe counterterm $a^{-2}O^{(0)}$

$$\frac{a^{-2}\langle O^{(0)} \rangle}{\langle O^{(2)} \rangle_U} \approx \frac{a^{-2}\langle \bar{\psi}\Gamma\psi \rangle}{\langle \bar{\psi}\Gamma\overleftrightarrow{D}\overleftrightarrow{D}\psi \rangle} \approx \frac{l^2}{a^2}, \quad (5.1)$$

where l is the typical $q\bar{q}$ separation. Our numerical work indicates that the ratio of Eq. (5.1) is actually quite small—of ~ 1 —so that the typical separation of the valence quarks l is about the same size as the lattice spacing $a \approx 0.2$ fm. Furthermore, the values of $R_U^{(2)}$ in Tables I and II indicate that the ρ is somewhat larger than the π , which is consistent with the analysis of meson wave functions.²² Nevertheless, both l 's might support the notion that the hadron is a tightly bound valence core surround-

ed by a pion cloud.²³ On the other hand, the shape of the distribution amplitude in Fig. 4, which hinges on the magnitude of the renormalized matrix element, might contradict the core picture. Assuming that the systematic errors inherent to the simulation have not misled us, the view that emerges from Fig. 4 is that the quarks range freely out to some surface, whose radius is presumably about 1 fm. This implies a somewhat larger $q\bar{q}$ separation than that implied by Eq. (5.1).

The surprisingly large values of $\tilde{A}_{\pi,\rho}^{(2)}$ have somewhat ambivalent implications. Our results indicate that the power-law divergences discovered in Ref. 5 are, in practice, quite bearable because they modify naive predictions by only 20–40%. Therefore, we can encourage the computation of the matrix elements needed for higher moments. On the other hand, the large values of the moments make the confrontation with experiments difficult since most observables depend on the distribution amplitude rather than a few low-order moments. Hence developing an interface between perturbative QCD and lattice QCD using the distribution amplitude formalism may require knowledge of many high-order moments (if they are large) in order to reconstruct the amplitude. Thus, it would be quite interesting to analyze the operators for the next moment $\tilde{A}^{(4)}$. As there are four derivatives in $\tilde{O}^{(4)}$ one will need a larger lattice and weaker coupling than in our calculation. Also, because of the counterterms, the $\tilde{O}^{(4)}$ calculation yields the ingredients needed to check our $\tilde{O}^{(2)}$ calculation, including its systematic errors. Even the sign of $\tilde{A}^{(4)}$ would be very significant, if our results are at least semiquantitative. If it opposes the first two terms of Eq. (4.1) the lattice calculations could become consistent with experiments. Otherwise, any chance of consistency would require still higher moments in Eq. (4.1). Finally, it would also be of great interest to repeat this calculation with dynamical fermions.

ACKNOWLEDGMENTS

We would like to thank Stan Brodsky, Peter Lepage, and Doug Photiadis for useful discussions on distribution amplitudes and phenomenology, and Paul Mackenzie and Hank Thacker for assistance with the numerical work. We thank the Computer Group at Fermilab for computer time on their VAX 11/780. This work has been supported in part by the National Science Foundation, and by the Department of Energy, under Contract No. DE-AT03-81ER-40029.

*Present address: Department of Physics, Indiana University, Bloomington, Indiana 47405.

†Present address: Theory Division-DESY, Notkestrasse 85, 2 Hamburg 52, Fed. Rep. of Germany.

¹As an example outside of the strong interactions, the determination of the CP -violating phase in the Kobayashi-Maskawa matrix requires a kaonic expectation value of $[\bar{s}\gamma_\mu(1-\gamma_5)d]^2$. C. Bernard, in *Gauge Theory on a Lattice*, edited by C. Zachos *et al.* (Argonne National Laboratory, Ar-

gonne, Illinois, 1984); A. Soni, in *Advances in Lattice Gauge Theory*, proceedings of the Tallahassee Conference, Florida State University, 1985, edited by D. W. Duke and J. F. Owens (World Scientific, Singapore, 1985).

²J. Polonyi and H. W. Wyld, *Phys. Rev. Lett.* **51**, 2257 (1983); G. Parisi in *Progress in Gauge Field Theory*, edited by G. 't Hooft *et al.* (Plenum, New York, 1984); G. G. Batrouni, G. R. Katz, A. S. Kronfeld, G. P. Lepage, B. Svetitsky, and K. G. Wilson, *Phys. Rev. D* **32**, 2736 (1985).

- ³E. Brooks *et al.*, Phys. Rev. Lett. **52**, 2324 (1984); N. H. Christ and A. E. Terrano, Nucl. Instrum. Methods **222**, 534 (1984); P. Bacilieri *et al.*, Report No. IFUP-TH 84/40, 1984 (unpublished); J. Beetem, M. Denneau, and D. Weingarten, IBM report, 1985 (unpublished).
- ⁴K. G. Wilson, Phys. Rev. **179**, 1499 (1969); W. Zimmerman, in *Lectures on Elementary Particles and Quantum Field Theory*, edited by S. Deser, M. Grisaru, and H. Pendleton (Brandeis University Press, Waltham, Mass., 1970), Vol. 1; R. A. Brandt, in *Highlights in Particle Physics*, edited by A. Zichichi (Editrice Compositori, Bologna, 1973).
- ⁵A. S. Kronfeld and D. M. Photiadis, Phys. Rev. D **31**, 2939 (1985).
- ⁶Even in the continuum power counting indicates divergences, but they vanish.
- ⁷*Handbook of Mathematical Functions*, edited by M. Abramowitz and I. Stegun (Dover, New York, 1970).
- ⁸G. P. Lepage and S. J. Brodsky, Phys. Rev. D **22**, 2157 (1980).
- ⁹S. Gottlieb, P. B. Mackenzie, H. B. Thacker, and D. Weingarten, Phys. Lett. **134B**, 346 (1984); Report Nos. Fermilab-PUB-84/98-T and UCSD-10P10-236 (unpublished).
- ¹⁰The + component is defined by, e.g., $p^+ = -p^0 + p^i$ for a meson traveling in the i direction. In the rest frame the i direction is arbitrary, so we have averaged over the three possible choices.
- ¹¹F. S. Acton, *Numerical Methods That Work* (Harper and Row, New York, 1980), p. 253.
- ¹²G. Parisi, S. Petrarca, and F. Rapuano, Phys. Lett. **121B**, 264 (1983).
- ¹³On the other hand, if we fit $M^{(2)}$ or $R_K^{(2)}$ to a straight line, we would obtain $A_\pi^{(2)} = \infty$ in the chiral limit. This would be absurd. Equations (2.5) and (2.7) suggest, however, that $M^{(2)}$ goes like K^n , $n \neq 1$.
- ¹⁴For example, F. Fucito, G. Martinelli, C. Omero, G. Parisi, R. Petronzio, and F. Rapuano, Nucl. Phys. **B210** [FS6], 407 (1982).
- ¹⁵V. L. Chernyak and A. R. Zhitnitsky, Nucl. Phys. **B201**, 492 (1982); Phys. Rep. **112**, 173 (1984).
- ¹⁶C. Bebek *et al.*, Phys. Rev. D **17**, 1963 (1978).
- ¹⁷Particle Data Group, Rev. Mod. Phys. **56**, S1 (1984) tabulates $\Gamma(\psi \rightarrow \pi^+ \pi^-)$ and $\Gamma(\psi \rightarrow e^+ e^-)$. A trivial calculation yields the form factor.
- ¹⁸S. J. Brodsky and G. P. Lepage, Phys. Rev. D **24**, 1808 (1981).
- ¹⁹For charged pions the factor g^2 in Eq. (4.2) is replaced by a sum of three terms, one of which is independent of g and which obscures the ϕ_π dependence of $\sigma / |F_\pi|^2$. See Ref. 18.
- ²⁰S. J. Brodsky (private communication).
- ²¹D. Weingarten, Nucl. Phys. **B215**, 1 (1983); H. Hamber and G. Parisi, Phys. Rev. D **27**, 208 (1983).
- ²²S. Gottlieb, *Advances in Lattice Gauge Theory* (Ref. 1).
- ²³In the quenched approximation the cloud would be composed of gluons, or glueballs, instead.